JEE Journal of Ecological Engineering

Journal of Ecological Engineering, 2027, 28(1), 346–363
https://doi.org/10.12911/22998993/xxxxx
ISSN 2299–8993, License CC-BY 4.0

Received: 2026.xx.xx
Accepted: 2026.11.16
Published: 2026.12.01

Physicochemical and energetic properties of biochars derived from leaves, branches, twigs, and mixtures obtained from urban pruning of *Ficus benjamina*

Segundo Alberto Vásquez Llanos[1*], Héctor Preciado del Castillo[1], Sebastian Huangal Scheineder[1], Magali Camila Vivas-Cuellar[2], Pedro Córdova-Mendoza[3], Karina Rivadeneira Sipion[4], Teresa Barrios Mendoza[5], Isis Córdova Barrios[3], Esteban Castellanos Borrero[6], Ada Patricia Barturén Quispe[1]

[1] Faculty of Chemical Engineering and Food Industries, Universidad Nacional Pedro Ruiz Gallo, Ciudad Universitaria, Calle Juan XXIII 391, Lambayeque 14000, Peru
[2] Biorefinery Research Group, Universidad Nacional de Ingeniería, Ciudad Universitaria, Avenida Túpac Amaru 210 Rímac, Lima 15333, Peru
[3] Faculty of Environmental and Sanitary Engineering, Universidad Nacional San Luis Gonzaga, Ciudad Universitaria, Avenida Los Maestros s/n, Ica 11004, Peru
[4] Faculty of Engineering, Universidad Tecnológica del Perú, Local Central, Prolongación Augusto B. Leguía con Avenida. Herman Meiner, Chiclayo 14001, Peru
[5] Faculty of Chemical and Petrochemical Engineering, Universidad Nacional San Luis Gonzaga, Ciudad Universitaria, Avenida Los Maestros s/n, Ica 11004, Peru
[6] Chemical Synthesis Research Group, Universidad Nacional Mayor de San Marcos, Ciudad Universitaria, Avenida Venezuela cuadra 34, Lima 15081, Peru
* Corresponding author's e-mail: svasquezll@unprg.edu.pe

ABSTRACT

Urban pruning residues constitute an underutilized source of lignocellulosic biomass, whose compositional heterogeneity may condition thermochemical conversion and the properties of biochar intended for energy applications. This study evaluated the physicochemical properties and energy performance of biochars obtained from leaves, branches, twigs, and their binary and ternary mixtures of pruning residues of *Ficus benjamina* L. Seven treatments were carbonized at 500 °C for 1 h under limited oxygen conditions. The biochars were characterized through proximate and elemental analysis, higher heating value (HHV), Fourier transform infrared spectroscopy (FTIR), atomic H/C and O/C ratios, and conversion and energy performance indicators. Mass yield ranged between 30.49 and 37.01%, and HHV ranged between 18.06 and 25.50 MJ/kg. The biochar obtained from the 50:50 mixture of branches and twigs (T3) presented the highest values of energy enrichment factor of 1.48 (EEF), energy yield of 47.95%, carbon densification factor of 1.52, calorific value improvement of 48.20%, combustibility index of 9.40 MJ/kg, and volatile ignitability of 23.51 MJ/kg. The biochar obtained from leaves (T7) achieved the highest mass yield but presented the lowest values of HHV, EEF, and energy yield, evidencing that a higher mass yield does not imply a higher energy recovery. FTIR and the H/C and O/C ratios evidenced the aromatization and condensation of the carbonaceous matrix, with loss of oxygenated functional groups. The proportion of leaves, branches, and twigs conditioned the physicochemical and energy properties of the biochars, evidencing differentiated profiles among treatments and their relevance for the thermochemical valorization of urban pruning residues.

Keywords: urban pruning biomass, *Ficus benjamina*, thermochemical conversion, fuel properties, biochar, waste valorization, energetic yield.

INTRODUCTION

The generation of waste derived from urban tree maintenance constitutes a growing challenge for municipal solid waste management, with an estimated global generation of nearly 47 kg of pruning residues per inhabitant per year (de Jesus Paula et al., 2025). In the specific case of *Ficus benjamina L.*, a fast-growing species widely used in urban tree planting, an approximate generation of 16 kg of pruning residues per tree has been estimated (Pérez-Arévaloa and Velázquez-Martí, 2018). Given this volume of residues, strategies such as recycling, direct incineration with energy recovery, and landfill disposal have been widely applied, but face relevant limitations: recycling is not applicable to all materials nor indefinitely, landfill disposal entails the loss of valorizable carbon-based resources, and incineration is energetically inefficient and generates greenhouse gases and toxic emissions that are costly to treat (Santos et al., 2026). In this context, pyrolysis constitutes an alternative thermochemical conversion route for the valorization of this type of residue. The physicochemical properties of the biochar obtained through this process are influenced by the characteristics of the feedstock and by the pyrolysis conditions employed. Specifically in urban pruning residues, carbonization has been reported to modify the heating value and energy yield of the resulting material relative to the parent biomass (Paudel et al., 2025).

Within this relationship between feedstock and biochar properties, pruning residues from a single tree do not constitute a homogeneous feedstock, since they incorporate plant parts with distinct biochemical composition from one another, a difference that is reflected in the products obtained when pyrolyzing each part of the tree separately. This was confirmed in a trial with parts of the same poplar tree, where biochar derived from leaves and bark showed lower energy performance than that of wood, due to the greater abundance of inorganic species in those plant parts, which limited the degree of aromatization achieved during pyrolysis (Qiu et al., 2023). In a complementary manner, the characterization of pruning residues of *Liquidambar styraciflua* determined a lignin content of 45% in bark, 28% in leaves, and 14% in branches, confirming compositional differences among fractions of the same individual, although without evaluating their pyrolytic behavior (Valdebenito et al., 2024). This compositional contrast is relevant for biochar formation, given that lignin generates a considerably higher solid char yield than cellulose and hemicellulose under equivalent pyrolysis conditions (Shahbaz et al., 2020).

This relationship between composition and solid carbon yield has also been evaluated among different sources of lignocellulosic biomass: in pruned apple tree branches, carbonization conditions affected the yield and fixed carbon content of the resulting biochar (X. Yang et al., 2020), and the comparison of pruning residues from apple, pear, and plum trees evidenced differences in heating value and ash content attributable to the species of origin (Kazimierski et al., 2021). In ornamental species, the evaluation of spring pruning residues from horse chestnut and black locust determined that their composition was suitable for use in pyrolysis processes aimed at obtaining biofuels and biomaterials (Taboada-Ruiz et al., 2024). In *Ficus benjamina*, a species used in urban tree planting, biochar production was evaluated from pruned branches at 400, 500, and 600 °C; the increase in carbonization temperature reduced energy yield and volatile content, while ash content (10.49–13.41%) and carbon content (66.71–68.93%) varied as a function of the temperature employed (Llanos et al., 2026).

In this species, the proportion of branches and leaves has shown an effect on the ash content, heating value, and flammability index of the unpyrolyzed biomass (Pérez-Arévalo and Velázquez-Martí, 2018), while its biochar has been characterized only from pruned branches subjected to different carbonization temperatures (Llanos et al., 2026). However, evidence on the relationship between the proportion of leaves, branches, and twigs, as well as their mixtures, and the properties of the resulting biochar in this species remains scarce; the available studies have focused mainly on the characterization of the biomass, without addressing its transformation into biochar. To address this gap, the objective of this study was to evaluate the influence of the proportion of leaves, branches, twigs, and their mixtures of pruning residues of *Ficus benjamina* on the mass yield, proximate composition, and energy properties of the biochars produced at 500 °C for 1 h. The results of this study provide evidence on the relationship between the compositional heterogeneity of *F. benjamina* pruning residues and the biochar response during thermochemical conversion, allowing the identification of how the

combination of woody and foliar fractions modifies mass recovery, energy concentration, and the characteristics of the product as a solid fuel. This information contributes to a more specific characterization of the pruning residues of this species and provides an experimental basis for evaluating its energy valorization from different feedstock compositions.

MATERIALS AND METHODS

Raw material preparation and treatment composition

The pruning residues of *Ficus benjamina L.* used in this study corresponded to the seven treatments previously characterized (Llanos et al., 2023), collected in public squares and urban green areas located along a high-traffic avenue in the city of Chiclayo, Peru. Following the same procedure described by those authors for the collection and preparation of the treatments, the pruning material was separated into three fractions: branches (B) of approximately 12±3 mm in diameter, twigs (T) of 2±0.5 mm in diameter, and leaves (L). The branches and twigs were cut into 100 mm fragments and dried in an oven at 105±5 °C for 24 h (Binder, model FD 115); additionally, the branches were longitudinally subdivided to increase the surface area exposed during carbonization. The leaves, in turn, were subjected to a pretreatment for the removal of surface impurities and to natural dehydration, prior to oven drying under the same conditions, and were subsequently ground and sieved through a Tyler 8 mesh for use in biochar production. From these three fractions, seven treatments were prepared with different proportions by weight, identified in the present study as T1 to T7: T1, 100% branches; T2, 100% twigs; T3, 50% branches and 50% twigs; T4, 40% leaves, 30% twigs, and 30% branches; T5, 50% leaves and 50% branches; T6, 70% leaves, 20% twigs, and 10% branches; and T7, 100% leaves. The seven treatments were stored in airtight bags until carbonization.

Preparation of biochars

Each treatment (T1–T7) was carbonized in three independent runs (21 experimental units, completely randomized design) under oxygen-limited conditions, using 100 mL porcelain crucibles. A 30 mL layer of pre-washed marine sand was placed at the bottom of each crucible, followed by 20 g of sample. The crucible was then filled to the rim with sand, sealed with aluminum foil, and closed with its lid. Washed marine sand (<150 µm) was used as a physical barrier to limit oxygen ingress into the crucible (Minatre et al., 2024). Oxygen concentration was not monitored; therefore, the atmosphere is considered oxygen limited rather than inert. Carbonization was performed in an electric muffle furnace (Thermolyne, Eurotherm 2116) set at 500 °C, without a programmable heating ramp. The furnace chamber reached 500 °C in approximately 38 min (average heating rate ≈ 12.5 °C min^{-1}), and the temperature was then held for 1 h (residence time). The crucibles were cooled inside the furnace for 24 h, then transferred to a desiccator and left to stand for 1 h before the biochar was recovered. The biochar was separated from the sand using a vibrating sieve for 3 min. It was then weighed, labeled according to its treatment (T1–T7), and stored in sealed plastic bags inside a desiccator until analysis. Prior to analysis, the biochars were ground to pass a 60-mesh sieve.

Proximate and elemental analysis

Moisture content (*M*), volatile matter (*VM*), and ash content (*Ash*) of the biochars from *Ficus benjamina* pruning residues (T1–T7) were determined following ASTM D3173, D3175, and D3174, respectively. Each biochar (three independent carbonization runs per treatment, n = 3) was analyzed once, and results are reported as mean ± standard deviation (SD) on an air-dried basis (ad). *M* was determined by drying 1 g of biochar at 105±5 °C for 4 h until constant mass (Equation 1). For *VM*, 1 g of undried biochar was heated in a covered crucible at 950±10 °C for 7 min in a preheated muffle furnace, and *VM* was calculated as the mass loss minus *M* (Equation 2). For *Ash*, 1 g of undried biochar was combusted in an uncovered crucible at 750±20 °C for 6 h (Equation 3). Fixed carbon (*FC*) was calculated by difference (Equation 4).

$$M\ (wt.\ \%) = (m_0 - m_1)/m_0 \times 100 \quad (1)$$

$$VM\ (wt.\ \%) = (m_2 - m_3)/m_2 \times 100 - M \quad (2)$$

$$Ash\ (wt.\ \%) = m_5/m_4 \times 100 \quad (3)$$

$$FC\ (wt.\ \%) = 100 - (\%\ M + \%\ VM + \%\ Ash) \quad (4)$$

where: m_0 and m_1 are the sample masses before and after drying; m_2 and m_3, before and after heating at 950 °C; and m_4 and m_5, the initial mass and the ash residue at 750 °C.

An elemental analysis was performed to quantify the carbon (*C*), hydrogen (*H*), nitrogen (*N*), and sulfur (*S*) content in the obtained biochars. The determination of C, H, and N was carried out using a CKIC 5E-CHN2200 elemental analyzer (ASTM 5373), while the sulfur content was quantified using the CKIC 5E-IRSII module (ASTM D4239). Each biochar (three independent carbonization runs per treatment, n = 3) was analyzed once, and results are reported as mean ± standard deviation (SD) on an air-dried basis (ad). The oxygen (*O*) content was calculated by difference, in accordance with Equation 5:

$$O\ (wt.\ \%) = 100 - (\%\ C + \%\ H + \%\ N + \%\ S + \%\ Ash) \quad (5)$$

The proximate and elemental composition of the unpyrolyzed biomass of each treatment was taken as the reference value (Llanos et al., 2023).

Analysis of higher heating value

The higher heating value (HHV) of each biochar (three independent carbonization runs per treatment, n = 3) was determined once using an isoperibol calorimeter (LECO AC600) following ASTM D5865-07. Samples were ground and pressed into pellets (0.5-1.0 g). Results are expressed as mean ± standard deviation (SD) on an air-dried basis (ad). The HHV of the unpyrolyzed biomass of each treatment was taken as the reference value (Llanos et al., 2023).

Mass yield and energy yield

The mass yield (*Y*, %) was calculated as the ratio between the mass of biochar obtained ($m_{biochar}$), weighed directly after separation from the sand, and the initial mass of biomass ($m_{biomass}$) subjected to carbonization, Equation 6:

$$Y\ (\%) = \frac{m_{biochar}}{m_{biomass}} \times 100 \quad (6)$$

Energy yield (*EY*, %) was calculated from the mass yield (*Y, %*) and the ratio between the HHV of the biochar (MJ/kg) determined experimentally in this study for each biochars and the HHV of the biomass (MJ/kg) of each treatment (Llanos et al., 2023), according to Equation 7:

$$EY\ (\%) = \frac{HHV_{biochar}}{HHV_{biomass}} \times Y \quad (7)$$

Indicators derived from energy and fuel performance

Energy enrichment factor (*EEF*) was calculated as the ratio between HHV of the biochar and that of the unpyrolyzed biomass, according to Equation 8 (Mbugua Nyambura et al., 2023):

$$EEF = \frac{HHV_{biochar}}{HHV_{biomass}} \quad (8)$$

The carbon densification factor (*CDF*) was calculated as the ratio between the carbon content of the biochar and that of the unpyrolyzed biomass, according to Equation 9 (Mbugua Nyambura et al., 2023):

$$CDF = \frac{C_{biochar}}{C_{biomass}} \quad (9)$$

Calorific value improvement (*CVI*) was calculated as the percentage increase in the higher heating value of the biochar relative to the unpyrolyzed biomass, according to Equation 10 (Mbugua Nyambura et al., 2023):

$$CVI = \left(\frac{HHV_{biochar}}{HHV_{biomass}} - 1\right) \times 100 \quad (10)$$

The fuel ratio (*FR*) was calculated as the ratio between fixed carbon and volatile matter of the biochars, according to Equation 11:

$$FR = \frac{Fixed\ carbon}{Volatile\ matter} \quad (11)$$

The combustibility index (*CI*, MJ/kg) and volatile ignitability (*VI*, MJ/kg) of the biochars were calculated using Equation 12 and Equation 13, respectively (Paudel et al., 2025):

$$CI = \frac{HHV}{FR} \times (115 - Ash) \times \frac{1}{105} \quad (12)$$

$$VI = \left[\frac{HHV - 0.338 \times FC}{VM+M}\right] \times 100 \quad (13)$$

Functional group analysis

Functional groups of biochars from treatments T1, T4, and T7 were evaluated by Fourier

transform infrared spectroscopy (FTIR). Spectra were obtained with a Perkin Elmer FTIR spectrometer, over a spectral range of 4000 to 500 cm^{-1} and a resolution of 16 cm^{-1}. Each spectrum corresponded to the average of 8 consecutive scans.

Min-Max normalization and statistical

The eight indicators of energy and fuel performance (fixed carbon, ash, mass yield, energy yield, higher heating value, fuel ratio, combustibility index, and volatile ignitability) were normalized using the Min–Max method, according to Equation 14:

$$x_{norm} = \frac{x - x_{min}}{x_{max} - x_{min}} \quad (14)$$

where: x corresponds to the observed value of each indicator for a given treatment, and x_{min} and x_{max} correspond to the minimum and maximum values observed for that indicator among the seven treatments evaluated.

The normalized values, ranging between 0 and 1, were represented by means of a radar chart, in order to comparatively visualize the relative profiles of the seven treatments. Differences among treatments (T1 to T7) for each response variable were evaluated by means of a one-way analysis of variance (ANOVA). Compliance with the assumptions of normality and homogeneity of variances was verified from the model residuals, by means of the Shapiro-Wilk and Levene tests, respectively. When both assumptions were met, comparisons among treatments were performed using Duncan's post hoc test. When either assumption was not met, the nonparametric Kruskal-Wallis test was applied, followed by Dunn's post hoc test. In all cases, differences were considered statistically significant when $p<0.05$. Statistical analyses and Min–Max normalization were performed using RStudio software, version 2024.04.1.

RESULTS AND DISCUSSION

Physicochemical properties of biochars

Proximate analysis of biochars

Carbonization at 500 °C substantially modified the proximate composition of the fractions evaluated. Compared with the precursor biomasses (Table 1), fixed carbon content increased from 8.33–12.62% to 40.58–63.23% in the biochars, while volatile matter decreased from 69.66–77.59% to 22.31–25.12% (Table 2). These variations are consistent with the loss of volatile compounds and the relative enrichment of the carbonaceous fraction during thermochemical conversion. Among the biochars, T1 presented the highest fixed carbon content (63.23%), followed by T3 (56.84%) and T2 (52.59%), while T7 recorded the lowest value (40.58%). The differentiation between the woody fractions and the foliar fraction is consistent with the higher lignin proportion reported for the woody parts of *Ficus benjamina*, estimated

Table 1. Proximate and elemental analysis and HHV of tree pruning of *Ficus benjamina*

Properties	B	T	B50T50	L40T30R30	L50B50	L70T20B10	L
Proximate analysis (wt.%)							
Moisture	6.40±0.05	7.40±0.01	7.67±0.09	8.39±0.01	8.53±0.02	8.90±0.03	9.44±0.01
Volatile matter	77.59±0.2	77.09±0.1	76.99±0.2	76.84±0.03	73.19±0.1	74.71±0.2	69.66±0.2
Ash	3.39±0.03	4.53±0.02	3.75±0.1	6.44±0.04	6.71±0.02	7.43±0.02	8.85±0.04
Fixed carbon	12.62±0.2	10.98±0.1	11.59±0.3	8.33±0.1	11.57±0.1	8.95±0.2	12.05±0.2
Elemental analysis (wt.%)							
Carbon	42.36±0.02	43.62±0.05	42.36±0.2	42.48±0.4	42.72±0.2	42.53±0.1	43.59±0.01
Hydrogen	6.15±0.2	5.84±0.02	5.85±0.02	5.55±0.05	5.93±0.04	5.86±0.09	5.86±0.04
Nitrogen	0.64±0.02	0.97±0.03	0.85±0.04	1.04±0.1	1.14±0.02	1.16±0.06	1.28±0.01
Sulphur	0.045±0.00	0.058±0.00	0.043±0.01	0.048±0.02	0.044±0.0	0.06±0.004	0.051±0.02
Oxygen	47.42±0.21	44.98±0.06	47.13±0.3	44.44±0.4	43.46±0.1	42.96±0.2	40.36±0.02
Higher Heating Value (MJ/kg)							
HHV	17.34±0.1	17.35±0.02	17.18±0.1	17.25±0.2	16.19±0.2	16.60±0.2	17.66±0.09

Note: B50T50: 50% of Branches and 50% of Twigs (Llanos et al., 2023).

at 29.6% for branches versus 22.85% for leaves (Pérez-Arévalo and Velázquez-Martí, 2018). Lignin exhibits a broader thermal degradation range than cellulose and hemicellulose, owing to the greater heterogeneity of its bonds and its aromatic structure, which favors a progressive decomposition during thermochemical treatment (Lu et al., 2021). The progressive thermal transformation of lignin contributes to the formation of condensed carbonaceous structures during carbonization (Waters et al., 2017).

Ash content also increased after carbonization and showed differences among the plant fractions, as shown in Tables 1 and 2. This increase in ash content is consistent with previous studies that attribute the concentration of the non-combustible mineral fraction of biochar to the loss of volatile matter during pyrolysis (Borges et al., 2025). In this regard, differences have been reported in the ash content of biochars obtained from branches and leaves of *Taxodium ascendens*, with average values of 4 and 13%, respectively (Zhang et al., 2024). Likewise, T7 presented an ash content higher than the range of 2.8–14.7% reported for biochars derived from poplar branches and bark, and slightly higher than the range of 21.2–27.2% obtained from leaves of the same species (Qiu et al., 2023). In *Eucalyptus* branch biochars produced at 500 °C, ash contents of 6.8–8.3% have been reported (Domingues et al., 2017), lower than those obtained for T1 (10.65%), T2 (20.46%), and T3 (16.42%). In urban pruning residues, a high proportion of ash has been observed in the precursor biomass (51.60%), while the resulting biochars presented contents between 15.40 and 38.61%, evidencing the variability of the mineral fraction between the feedstock and the carbonized products (de Jesus Paula et al., 2025). Similarly, in biochars obtained through slow pyrolysis of mixed tree leaves, ash content ranged between 4.58 and 12.75% and increased with pyrolysis temperature, along with the increase in fixed carbon (Ibitoye et al., 2025).

The differences observed across studies could be associated with the species, the plant fraction, the mineral composition, and the conditions of the biomass source. In the present study, the trend observed between T1 and T7 indicates that the incorporation of leaf fractions increased the mineral load of the biochar and, consequently, its ash content.

Elemental analysis of biochars

Elemental analysis evidenced a relative carbon enrichment in the biochars relative to the precursor biomasses. T1 and T3 recorded the highest carbon contents, with 67.67 and 64.65%, respectively, while T7 presented the lowest value (50.41%). In contrast, hydrogen content decreased from 5.55–6.15% in the biomasses to 2.12–2.31%

Table 2. Proximate and elemental analysis of the biochars (T1–T7), air-dried basis

Properties	T1	T2	T3	T4	T5	T6	T7
Proximate analysis (wt.%)							
Moisture	3.47±0.003	4.04±0.098	4.43±0.20	5.76±0.055	5.45±0.036	4.93±0.04	5.48±0.05
Volatile matter	22.65±0.05	22.91±0.38	22.31±0.2	22.90±0.26	23.75±0.34	24.40±0.07	25.12±0.07
Ash	10.65±0.03	20.46±0.12	16.42±0.2	23.44±0.78	21.80±0.08	24.35±0.05	28.82±0.08
Fixed carbon	63.23±0.05	52.59±0.55	56.84±0.5	47.90±0.48	49.00±0.44	46.32±0.05	40.58±0.05
Elemental analysis (wt.%)							
Carbon	67.67±0.1	58.39±0.95	64.65±0.7	57.38±0.4	59.04±0.04	54.66±0.1	50.41±0.03
Hydrogen	2.30±0.04	2.28±0.02	2.30±0.03	2.12±0.01	2.30±0.02	2.31±0.00	2.29±0.006
Nitrogen	0.77±0.05	0.88±0.006	0.69±0.03	0.89±0.05	0.98±0.02	1.07±0.02	1.18±0.03
Sulphur	1.39±0.02	0.16±0.006	0.16±0.01	0.12±0.01	1.33±0.06	1.17±0.06	1.27±0.08
Oxygen	17.22±0.2	17.83±0.9	15.78±0.5	16.05±0.9	14.55±0.01	16.44±0.14	16.03±0.1
Molar ratios							
O/C	0.19±0.00	0.23±0.02	0.18±0.01	0.21±0.01	0.18±0.00	0.22±0.00	0.24±0.00
H/C	0.41±0.01	0.47±0.01	0.43±0.01	0.44±0.01	0.47±0.00	0.51±0.00	0.55±0.00
Higher Heating Value (MJ/kg)							
HHV	25.24±0.1ab	22.74±0.4ab	25.5±0.03b	22.19±0.1ab	21.72±0.1ab	19.96±0.04ab	18.06±0.03a

Note: Values are mean ± SD (n = 3 independent carbonization runs). Different letters in a row indicate significant differences ($p<0.05$, Dunn's test).

in the biochars. Consequently, the atomic H/C and O/C ratios ranged between 0.41–0.55 and 0.18–0.24, respectively (Table 2), and the seven biochars shifted toward lower values of both ratios in the Van Krevelen diagram (Figure 1), relative to the reference lignocellulosic biomass.

T1 and T3 presented the lowest relative H/C positions, with 0.41 and 0.43, respectively, while T7 reached the highest value (0.55). This behavior, in which the woody fractions present lower H/C values than the foliar material, is consistent with the pattern reported in the literature, although at higher pyrolysis temperatures (750 °C), where branches attain a greater degree of structural aromatization than leaves (Zhang et al., 2024). The reduction in the H/C and O/C ratios is consistent with the removal of hydrogen and oxygen during thermochemical conversion through dehydration, decarboxylation, and dehydrogenation reactions (Kujawska et al., 2026). These processes favor the relative enrichment of carbon and the development of carbonaceous structures of greater aromatic character in lignocellulosic materials subjected to pyrolysis (Zhang et al., 2024). Likewise, these H/C and O/C ratios would reflect the structural transformations and changes in the surface hydrophilicity of the biochar, associated with a greater degree of carbonization and with the loss of oxygenated and hydrogenated functional groups, such as hydroxyl and carboxyl groups, at higher temperatures, which would be indicative of a surface of more aromatic character (Zhao et al., 2017).

Higher heating value

The higher heating value (HHV) ranged between 18.06 and 25.50 MJ/kg (Table 2), with significant differences among treatments (Kruskal-Wallis, $\chi^2 = 19.636$; $p<0.05$). The differences in HHV were associated with the composition of the biochars. T3 and T1, with HHV of 25.50 and 25.24 MJ/kg, presented elemental carbon contents of 64.65 and 67.67% and ash contents of 16.42 and 10.65%, respectively. In contrast, T7 recorded the lowest elemental carbon content (50.41%), the highest ash content (28.82%), and the lowest HHV (18.06 MJ/kg) (Table 2). This trend is consistent with the influence of elemental and proximate composition on the energy content of biochar. It has been evidenced that FC contributes significantly to the prediction of HHV and that both elemental carbon and ash content are involved in its variation (Qian et al., 2020), and that a high ash content has been associated with lower calorific values in biochars, while the energy properties of lignocellulosic materials depend on their elemental composition and precursor material (Borges et al., 2025; Kazimierski et al., 2021).

This dependence on the precursor material is manifested among tissues of the same tree: in poplar biochars obtained at 400 and 600 °C, HHV was 24.3–26.7 MJ/kg in wood, 23.2–24.4 MJ/kg in bark, and 18.2–21.2 MJ/kg in leaves, a difference attributed to the greater abundance of inorganic species in bark and leaves, which

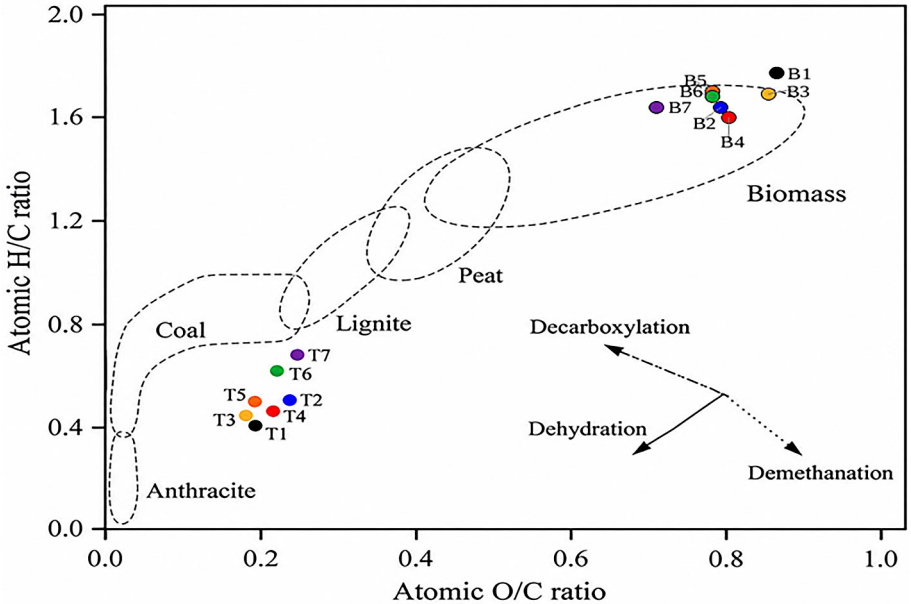

Figure 1. Van Krevelen diagram of *Ficus benjamina* biochars. Note: The compositional regions were adapted from (Leng et al., 2020)

hinders the aromatization of the biochar (Qiu et al., 2023). This same trend is confirmed when comparing organs of *Flourensia oolepis* biomass, in which stem biochar reached 23.6 MJ/kg versus 19.9 MJ/kg in leaves, consistent with fixed carbon contents of 86.1 and 79.1%, respectively (Silva et al., 2017). Branches and twigs, owing to their higher proportion of lignified tissue, tend to generate biochars with higher carbon content and aromatic structure, given that lignin is the main contributor to the solid fraction, whose char conversion yield (48.8%) considerably exceeds that of hemicellulose (21.1%) (Cao et al., 2014). In a complementary manner, the inorganic fraction acts as an inert diluent of the combustible carbon: woody biochars record ash contents below 7%, compared with values that can exceed 50% in non-woody biochars (Tomczyk et al., 2020).

The values obtained for T1 and T3 fell within the ranges reported for wood and bark, while T7 presented an HHV close to the range reported for leaves. These values are also consistent with those reported for pruned branches of *Ficus benjamina* carbonized between 400 and 600 °C, whose HHV ranged between 24.23 and 26.07 MJ/kg with ash contents of 10.49 to 13.41% (Llanos et al., 2026), a range that includes the value obtained for T1. Similarly, biochars from leaves of different species have recorded HHV between 20 and 28 MJ/kg, with the highest values corresponding to leaves with higher fixed carbon and lower ash content, and the lowest values to those with lower fixed carbon and higher mineral fraction (Yao et al., 2018), a pattern consistent with the lower HHV and higher ash content observed in T7. In contrast, biochar from mixed tree leaves obtained by slow pyrolysis reached values of up to 23.32 MJ/kg, with increases in fixed carbon, ash, and carbon content with temperature, in parallel with the decrease in biochar mass yield (Ibitoye et al., 2025), higher than that recorded in T7, which could be related to differences in the specific composition of *Ficus benjamina* leaves or to the particular carbonization conditions employed in this study. The participation of plant fractions in the mixtures was also reflected in the energy behavior. T4, with 60% woody fractions, presented an HHV of 22.19 MJ/kg, while T6, with 70% foliar fraction, recorded 19.96 MJ/kg, a value close to that obtained for T7 (18.06 MJ/kg). This behavior is consistent with the physicochemical differences reported between biochars derived from branches and leaves (Campos et al., 2020).

Taken together, the variation in HHV at 500 °C for one hour is explained by the convergence of three factors: the lignocellulosic composition of the precursor, which governs the yield and aromaticity of the residual char; the inorganic matter content, which dilutes the combustible fraction; and the degree of devolatilization achieved, which determines the final proportion of fixed carbon in the carbonized material.

Characterization by FTIR spectroscopy

The FTIR spectra of biochars T1 (100% branches), T4 (40% leaves with 30% twigs and 30% branches), and T7 (100% leaves) presented differences in the position and relative intensity of the absorption bands (Figure 2).

In the 3600–3200 cm^{-1} region, transmittance minima were observed at 3532 cm^{-1} (T1), 3334 cm^{-1} (T4), and 3420 cm^{-1} (T7). These positions fall within the region associated with O–H vibrations; in biochars from pruning residues, signals around 3600 and 3350 cm^{-1} have been identified and associated with these vibrations (Anđelini et al., 2023). Likewise, the 3500–3280 cm^{-1} region has been related to H–O···H hydrogen bonds in pyrolysis processes of lignocellulosic biomass (H. Yang et al., 2020). In the 3100–3000 cm^{-1} range, minima were identified at 3018, 3034, and 3060 cm^{-1} for T1, T4, and T7, respectively. These signals are located within the spectral range to which the C–H stretching of aromatic structures has been assigned, reported around 3000–3100 cm^{-1} in biochars obtained from pruning residues (Anđelini et al., 2023). The correspondence is closer for T4, whose minimum was recorded at 3034 cm^{-1}, close to the 3030 cm^{-1} signal attributed to the C–H of aromatic structures, whereas the C–H stretching of aliphatic chains has been associated with signals of lower wavenumber, around 2955, 2920, and 2895 cm^{-1} (H. Yang et al., 2020).

In the 1700–1500 cm^{-1} region, modifications in the spectral profile were observed, while the minima close to 1486 cm^{-1} (T1), 1422 cm^{-1} (T4), and 1476 cm^{-1} (T7) fall within the region in which C=C vibrations and C–H deformations have been described in biochars from pruning residues (Prelac et al., 2023). Signals close to 1690 cm^{-1} have also been related to aromatic structures and C=C bonds in pruning biochars (Anđelini et al., 2023). Between 1300 and 1000 cm^{-1}, the minima at 1038 cm^{-1} (T1), 1110 and 1022 cm^{-1} (T4), and 1100 cm^{-1} (T7) were located within the region

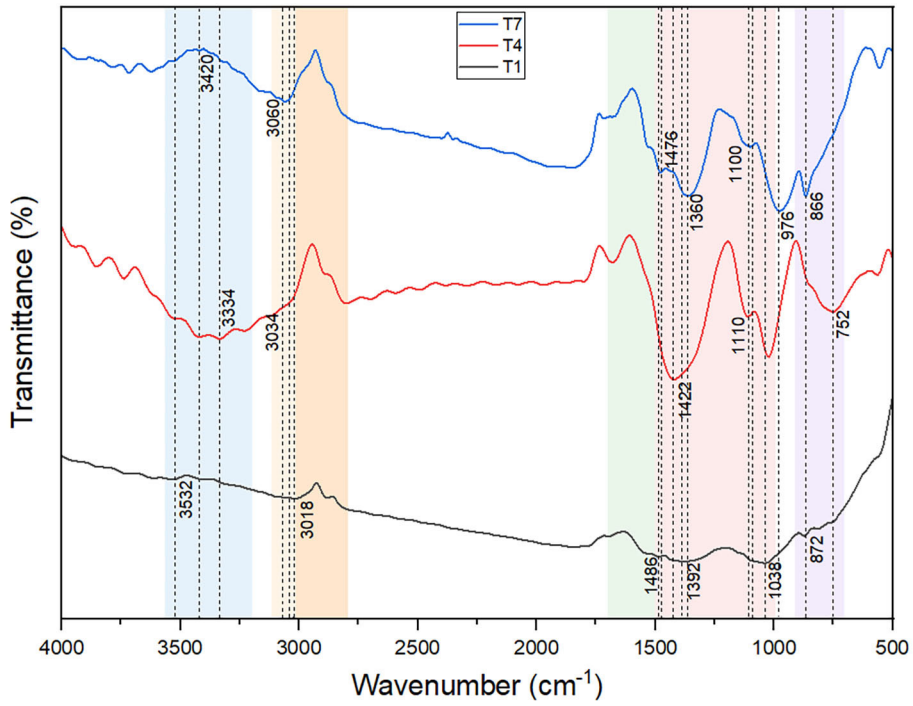

Figure 2. FTIR spectra of selected *Ficus benjamina* biochars

associated with C–O vibrations (Prelac et al., 2023). In the lower wavenumber zone, T1 and T7 presented signals at 872, 752, and 866 cm^{-1}, respectively, all of which fall within the 900–700 cm^{-1} region associated with C–H deformations of aromatic structures. The proximity of these signals to the positions of 873 and 750 cm^{-1} related the positive cross-peaks observed at 873, 843, 811, and 750 cm^{-1} to a common behavior of polysubstituted aromatic groups during the pyrolysis of cellulose (H. Yang et al., 2020).

The spectral differences among T1, T4, and T7 show that the composition of branches, leaf-twig mixture, and branches was reflected in the distribution of detectable functionalities. This variability is consistent with the influence of pyrolysis temperature, biochar H/C ratio, and ash content on the FTIR signals of biochars (Janu et al., 2021). Nevertheless, the FTIR evidence should be interpreted jointly with the H/C and O/C ratios, given that the decrease in these ratios during pyrolysis is related to the removal of aliphatic structures and the increase in aromaticity and ring condensation (Mafu et al., 2017).

The plant composition of the precursor biomass was associated with differences in the physicochemical and energy properties of the biochars obtained under the same carbonization condition. The treatments with greater participation of woody fractions presented, in general terms, higher fixed carbon and elemental carbon contents and lower ash contents than the biochar obtained exclusively from leaves (Table 2). This trend was reflected in HHV, which ranged between 18.06 and 25.50 MJ/kg, with the highest value in T3 and the lowest in T7. The FTIR characterization of the selected biochars complemented the compositional analysis through the identification of oxygenated, aliphatic, and aromatic functionalities in the carbonized matrix.

Production yield and energy performance of biochars

Mass yield

The mass yield of the biochars ranged between 30.49±0.18% (T1) and 37.01±0.53% (T7). Statistically significant differences were determined among treatments ($F(6,14) = 200.6$; $p<0.05$), according to the analysis of variance. Duncan's multiple comparison test ($\alpha = 0.05$) showed differences among treatments, showed in Table 3. These values fall within the range reported for the carbonization of pruned *Ficus benjamina* branches, whose biochars presented mass yields of 34.32, 31.20, and 28.59% at 400, 500, and 600 °C, respectively, after 2 h of carbonization (Llanos et al., 2026). In woody pruning residues of other species, carbonization of apple tree

branches at 500 °C produced yields close to 30% (X. Yang et al., 2020). Likewise, the decrease in mass yield with increasing pyrolysis temperature, attributed to greater degradation of organic matter and release of volatile components, has been reported for residues of different fruit species (Kazimierski et al., 2021). In another study with grapevine pruning residues, biochar production at 500 °C for 1 h presented yields close to 30%, confirming that this range can be obtained under pyrolysis conditions of lignocellulosic pruning residues (Anđelini et al., 2023). The difference observed between T1 and T7, under the same carbonization temperature and time, indicates that the recovery of the solid fraction varied among the plant compositions evaluated. Differences in the biochemical and mineral composition among leaves, branches, and bark can modify their behavior during thermochemical conversion and the distribution of pyrolysis products (Qiu et al., 2023). In urban pruning residues of *Liquidambar styraciflua*, compositional differences between leaves and branches have also been identified, associated with differentiated thermal behaviors during thermochemical conversion (Valdebenito et al., 2024). The heterogeneity in the yield of urban pruning residues is explained fundamentally by the balance between the recalcitrance of lignin in branches and the catalytic effect of ash in leaves (Qiu et al., 2023; Sun et al., 2017).

Energy enrichment factor

The energy enrichment factor (EFF) ranged between 1.02±0.006 and 1.48±0.012, with significant differences among treatments (Kruskal-Wallis, $\chi^2 = 19.418$; $p<0.05$). Dunn's multiple comparison test ($\alpha = 0.05$) showed differences among treatments (Table 3). EEF values higher than 1 indicate improved energy densification (Mbugua Nyambura et al., 2023)**.** Woody fractions tend to generate biochars of higher fuel quality than non-woody fractions, owing to their higher lignin content, a precursor of condensed aromatic structures associated with a higher EEF (Borges et al., 2025). In contrast, leaves present a higher proportion of inorganic species, which favors gasification reactions, limits aromatization, and reduces both the HHV and the EEF of the resulting biochar (Qiu et al., 2023); likewise, a higher ash content would hinder the formation of fixed carbon (Sun et al., 2017).

The increase in EEF observed after carbonization is consistent with studies conducted on pruning residues. Pyrolysis of apple, cherry, and pear tree branches produced increases in heating value, on average 62% (EEF: 1.61), compared with the original biomasses during the thermal treatment (Saletnik et al., 2021). In pruning residues of apple, pear, and plum trees, an increase in EEF within the range of 1.56 to 2.44 was also observed in the pyrolysis products, accompanied by a higher carbon content at higher temperatures (Kazimierski et al., 2021), a range that is comparable to, although higher than, that obtained in the present study (1.02–1.48). Although a higher pyrolysis temperature raises the HHV and the EEF of biochar, this effect is usually accompanied by a reduction in the solid yield and in the overall energy yield of the process (Ibitoye et al., 2025). The difference between T3 and T7 is consistent with this pattern: the lower EEF of T7 (100% leaves) would be associated with its higher content of inorganic species and lower lignin contribution, while the higher EEF of T3 (branches and twigs) would reflect a woody fraction with greater aromatization potential, consistent with the variation previously observed in the carbon content and HHV of the treatments.

Energy yield

The energy yield (EY) ranged between 37.84±0.45% (T7) and 47.95±0.34% (T3), with

Table 3. Mass and energy yield indices of *Ficus benjamina* biochars

Indicator	T1	T2	T3	T4	T5	T6	T7
Y, %	30.49±0.18f	34.31±0.085c	32.36±0.20e	34.51±0.22c	33.84±0.13d	35.56±0.20b	37.01±0.53a
EEF	1.45±0.012ab	1.31±0.021ab	1.48±0.012b	1.30±0.010ab	1.35±0.01ab	1.20±0.02ab	1.02±0.006a
EY, %	44.40±0.60c	44.99±0.79bc	47.95±0.34a	44.83±0.17bc	45.64±0.41b	42.76±0.38d	37.84±0.45e
CDF	1.60±0.003	1.34±0.022	1.52±0.011	1.35±0.005	1.38±0.006	1.29±0.005	1.16±0.00
CVI, %	45.59±1.18	31.11±2.22	48.20±0.85	29.90±1.15	34.86±1.14	20.25±1.60	2.24±0.64

Note: Values are mean ± SD (n = 3 independent carbonization runs). Different letters in a row indicate significant differences ($p<0.05$).

statistically significant differences among treatments ($F(6,14) = 127.9$; $p<0.05$). Duncan's test ($\alpha = 0.05$) showed differences among treatments according to the groupings presented in Table 3. In pruned branches of *Ficus benjamina*, energy yield decreased from 51.6±0.15% to 39.36±0.48% as carbonization temperature increased from 400 to 600 °C, over 2 h; the biochars obtained at 400 and 500 °C presented higher EY, associated with their higher carbon contents and lower ash contents, as well as with higher heating values (Llanos et al., 2026). A greater contribution of woody fractions tends to favor energy yield, owing to their more stable lignocellulosic structure and lower ash content, whereas herbaceous or non-woody fractions present lower thermal stability, which translates into energetically less robust carbonized products (Cárdenas-Aguiar et al., 2024). In biochars obtained from bamboo and wood mixtures, values of 44.77–48.73% were reported under different pyrolysis conditions (Gao et al., 2022). The variation in EY among the treatments evaluated thus reflects the combination of the mass conserved during carbonization and the energy content achieved by the solid product, which is consistent with what has been reported for forest and agricultural residues, where energy yield followed a trend similar to that of biochar yield (X. Yang et al., 2017).

Carbon densification factor

The carbon densification factor (CDF) ranged between 1.16±0.00 (T7) and 1.60±0.003 (T1) (Table 3). A CDF value above 1 indicates carbon enrichment, a value equal to 1 indicates, in theoretical terms, the absence of net change, while a value below 1 would suggest carbon dilution or the possible presence of analytical artifacts (Wang, 2026). The distribution of CDF was consistent with the elemental carbon contents determined previously, where T1 and T3 presented the highest values and T7 the lowest carbon content. In molded biochars obtained from mixtures of bamboo and *Chinese fir*, the increase in pyrolysis temperature produced increases in carbon content and CDF, while the H/C and O/C ratios decreased (Gao et al., 2022). Similarly, biochars derived from different biomass components (leaf, wood, and bark) of trees of the species *Eucalyptus polybractea* (pyrolysis at 300 to 500 °C, for 30 min) showed significant differences in their fuel quality and ash properties, attributable to the distinct structural composition of each fraction (Abdullah et al., 2010). A high initial carbon content in the feedstock does not guarantee greater carbon recovery; instead, wood density and the structural stability derived from lignin dominate retention outcomes, and in interspecific studies, tree species and their functional traits jointly determine the efficiency of carbon fixation during slow combustion (Wang, 2026). This relationship between carbon enrichment and CDF is consistent with the distribution observed in the present study, particularly in T1 and T3, which presented the highest relative carbon contents and CDF values.

Calorific value improvement

The calorific value improvement (CVI) ranged between 2.24±0.64% (T7) and 48.20±0.85% (T3), while T1 presented a value of 45.59 ± 1.19% (Table 3). The magnitude of the CVI expresses the percentage increase in the HHV of the biochar relative to the precursor biomass. In bamboo and Chinese fir mixtures, increases in heating value of 64.73–70.79% were reported after pyrolysis, accompanied by an increase in carbon content and CDF (Gao et al., 2022). The difference between T3 and T7 was consistent with the observed behavior. T3 presented the highest CVI, while T7 recorded the lowest increase. This correspondence between EEF and CVI indicates that the treatments that achieved a greater relative improvement in heating value also presented a greater energy densification. In pruning residues of fruit trees, the increase in the heating value of biochars relative to the precursor biomasses has also been associated with thermochemical transformation and the relative carbon enrichment of the solid product (Saletnik et al., 2021).

The results show that the pruning fractions and their combinations presented differentiated responses in terms of mass yield, EEF, EY, CDF, and CVI. The joint variation of these indicators demonstrates that the energy performance of biochar was not determined solely by the amount of solid product recovered, but also by the concentration of carbon and energy achieved during carbonization. Indeed, T1 presented the highest CDF, while T3 achieved the highest CVI, evidencing that both indicators describe related, but not equivalent, dimensions of the energy performance of the solid product.

Relationship between fixed carbon and higher heating value of biochars

Fixed carbon (FC) showed a significant, positive linear association with the higher heating value (HHV) of the seven biochars from *Ficus benjamina* ($r = 0.941$; $p<0.05$; Figure 3). T7 simultaneously presented the lowest FC content (40.58%) and HHV (18.06 MJ/kg), while T1 and T3 recorded the highest FC contents (63.23 and 56.84%, respectively) and elevated HHV values (25.24 and 25.50 MJ/kg). The concentration of FC in biochars derived from pruning residues depends on the composition of the feedstock and on the carbonization conditions (Sun et al., 2017). In pruned apple tree branches, the increase in carbonization severity significantly modified FC content (X. Yang et al., 2020). Although the association between FC and HHV was positive and significant, T3 presented the highest HHV (25 MJ/kg), while T1 recorded the highest FC content (63.23%), indicating that the variation in HHV among treatments was not specifically determined by FC. A differential behavior between FC and HHV has also been observed in densified materials made from urban pruning residues (Petricoski et al., 2020). Taken together, the observed association confirms the relationship between FC concentration and the HHV of biochars, but the difference between T1 and T3 indicates that HHV is also conditioned by other physicochemical characteristics of the product.

Performance indices of biochar as solid fuel

Fuel ratio

The fuel ratio (FR) ranged between 1.62±0.006 (T7) and 2.79±0.006 (T1). Statistically significant differences were determined among treatments (Kruskal-Wallis, $\chi^2 = 19.362$; $p<0.05$); Dunn's test ($\alpha = 0.05$) showed differences among treatments according to the groupings presented in Figure 4. Among the treatments evaluated, T1–T5 presented FR values above 2.0, while T6 and T7 recorded values below this level, with potential to be used as industrial fuels. In coal-fired power plants, coals with an FR in the range of 0.5 to 3 are commonly used; however, an FR higher than 2 causes ignition problems and flame instability (Ayaa et al., 2025), in addition to the fact that a higher FR results in lower emission of volatile pollutants, such as NOx and SOx (Mbugua Nyambura et al., 2023). Unlike these reference fossil fuels, urban pruning residues, composed of leaves and thin branches, naturally present, without thermal treatment, a low FR, associated with their high volatile matter content and low fixed carbon. In pyrolyzed oak pruning residues, an FR of 2.66 has been reported, one of the lowest values among different types of carbonized biomass (Borges et al., 2025).

In the present study, FR decreased consistently with the increase in the proportion of leaves

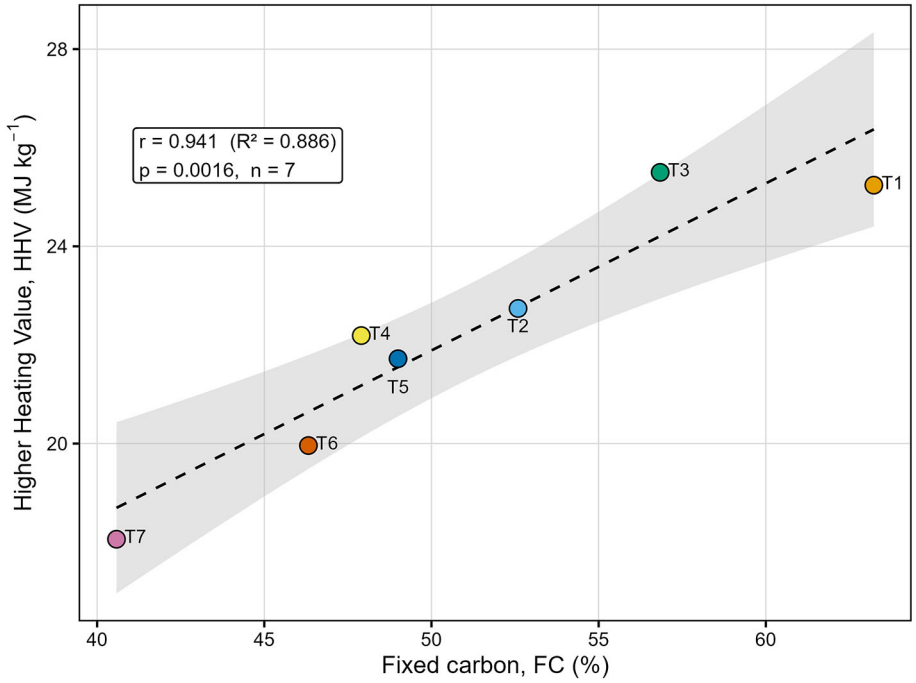

Figure 3. Correlation between FC and HHV of *Ficus benjamina* biochars

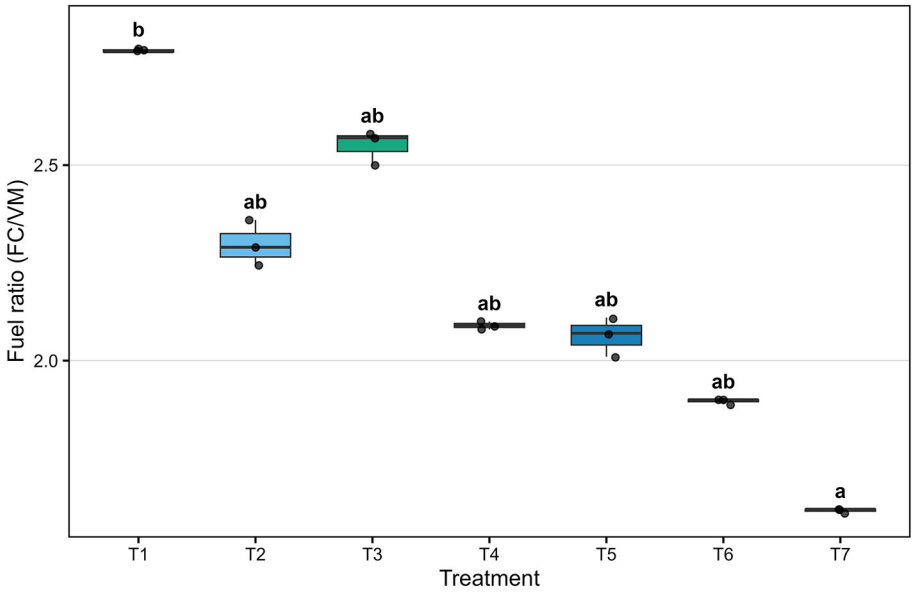

Figure 4. Fuel ratio of *Ficus benjamina* biochars. Note: different letters indicate significant differences ($p<0.05$, Dunn's test).

in the mixture, from 2.79 in T1 (100% branches) to 1.62 in T7 (100% leaves), with intermediate values in the treatments with binary and ternary mixtures. This gradient would be attributable to the lower content of inorganic species and the greater structural stability of the woody fractions, consistent with what has been reported for biochars from wood, bark, and leaves of the same tree species, where the woody fractions systematically presented lower ash content than the leaves (Abdullah et al., 2010; Saletnik et al., 2021). It is worth noting that T4 and T5, which combine leaves with woody fractions, presented FR values slightly lower than expected from a proportional combination of their pure components, while T3 and T6 were positioned slightly above, suggesting that the effect of the mixture on FR would not be strictly additive. Nevertheless, FR alone does not allow combustibility to be defined, owing to the differences in the functional groups present in the FC and VM fractions (Luthfi et al., 2024); therefore, its interpretation should be complemented with the proximate composition and the chemical characterization of the carbonaceous and volatile fractions (Santos et al., 2026). A high FR could hinder ignition and slow down combustion, resulting in greater amounts of unburned carbon and lower combustion efficiency; in contrast, biochars with lower FR could offer greater combustibility and better flame stability, although with a higher risk of unintentional ignition during storage (Mbugua Nyambura et al., 2023).

Combustibility index

The combustibility index (CI) ranged from 8.92±0.12 MJ/kg (T2) to 9.40±0.17 MJ/kg (T3) (Figure 5a). Statistically significant differences were determined among treatments ($p<0.05$). Duncan's post hoc test ($\alpha = 0.05$) showed significant differences among treatments. All seven treatments presented values below the optimal reference range of 12.56 to 23.02 MJ/kg, an interval used to assess the compatibility of solid fuels with coal co-combustion processes (Park et al., 2025). The highest values corresponded to the blends T3, T5, and T4, whereas the pure fractions of branches (T1) and twigs (T2) were among the lowest. The CI simultaneously integrates HHV, FR, and ash content; therefore, its response does not depend solely on HHV and may decrease as FR increases, even when the calorific value rises (Paudel et al., 2025). In the present study, the CI did not replicate the woody-to-foliar gradient of FR (2.79 in T1 to 1.62 in T7), which is consistent with the higher FR of T1 reducing the HHV/FR quotient, whereas the lower FR of T7 would partially offset its lower HHV, thereby compressing the differences among treatments. Similarly, in biomass residues subjected to torrefaction, a reduction of the CI associated with an increase in FR has been observed, owing to the higher relative concentration of fixed carbon and the lower proportion of volatile matter (Conag et al., 2017).

The CI value for urban pruning residues of *Ginkgo biloba* was 80.02 MJ/kg, then, after pyrolysis at 400, 500, and 600 °C for 1 h, it decreased after pyrolysis at 400, 500, and 600 °C for 1 h to 13.69, 9.97, and 5.80 MJ/kg, respectively (Paudel et al., 2025); the value at 500 °C is of the same order as the maximum recorded in the present study (T3, 9.40 MJ/kg). In this regard, the proximate composition, particularly the fractions of fixed carbon, volatile matter, and ash, conditions the energetic behavior of biochars and their response as solid fuels (Borges et al., 2025). Lower CI values may lead to slower combustion performance and lower mass consumption during the combustion process due to the lower volatile content (Paudel et al., 2025). In the treatments studied, CI values below this range indicate that, under this specific criterion, none reached the reference range for co-combustion, even though some treatments presented high HHV values. However, the CI of solid fuels can also be evaluated using the volatile ignitability, considered an alternative measure to the CI (Conag et al., 2017).

Volatile ignitability

The volatile ignitability (VI) ranged from 14.19±0.09 MJ/kg (T7) to 23.51±0.41 MJ/kg (T3) (Figure 5b).

Statistically significant differences were determined among treatments ($p<0.05$). Duncan's post hoc test ($\alpha = 0.05$) showed significant differences among treatments. As shown in Figure 5b, T3 and T4 exhibited the highest VI values, while T7 recorded the lowest value and was the only treatment below the reference value of 14.5 MJ/kg. The difference between both treatments coincides with their differences in HHV and proximate composition. VI is used as an indicator associated with the combustion characteristics of carbonized materials. VI values between 17.60 and 18.05 MJ/kg were reported for biochars obtained from peanut shell and sugarcane bagasse, considering 14.5 MJ/kg as the reference value for this indicator (Hadey et al., 2022). Compared with this criterion, the results shown in Figure 5b evidence that T1–T6 exceeded this value, although T1 and T6 were close to the threshold, while T7 presented a slightly lower VI. The higher VI of T3 is consistent with its higher HHV, while the lower VI of T7 coincides with its lower energy content; however, this indicator should be interpreted jointly with the proximate composition and the other energy properties of the fuel. The differences among the various fractions of the biomass of the same tree were reflected in the combustion properties of the biochars obtained, which supports the influence of the composition of the precursor material on the characteristics of the carbonized product (Qiu et al., 2023). In this regard, the differences observed among treatments suggest that the various fractions of *Ficus benjamina* pruning residues influenced VI, with T3 standing out for presenting the highest value of this indicator under the conditions evaluated.

Overall, FR, CI, and VI showed distinct responses across the evaluated formulations. T1 exhibited the highest FR, whereas T3 achieved the highest CI and VI values. T7 showed the lowest FR, CI, and VI values, consistent with its lower FC and lower HHV. The combined variation of these indicators confirms that the composition of

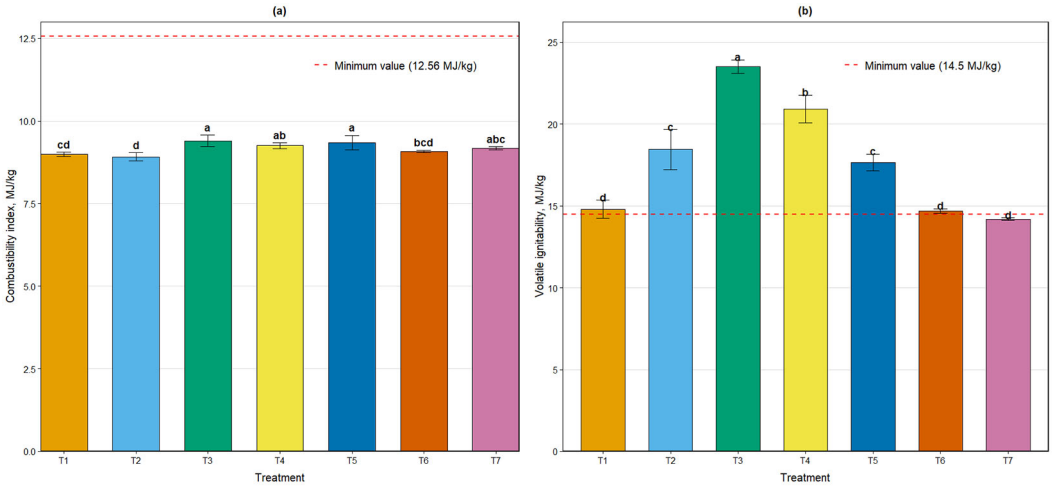

Figure 5. (a) Combustibility index of biochars; (b) Volatile ignitability of biochars. **Note:** different letters indicate statistically significant differences ($p<0.05$, Duncan's test)

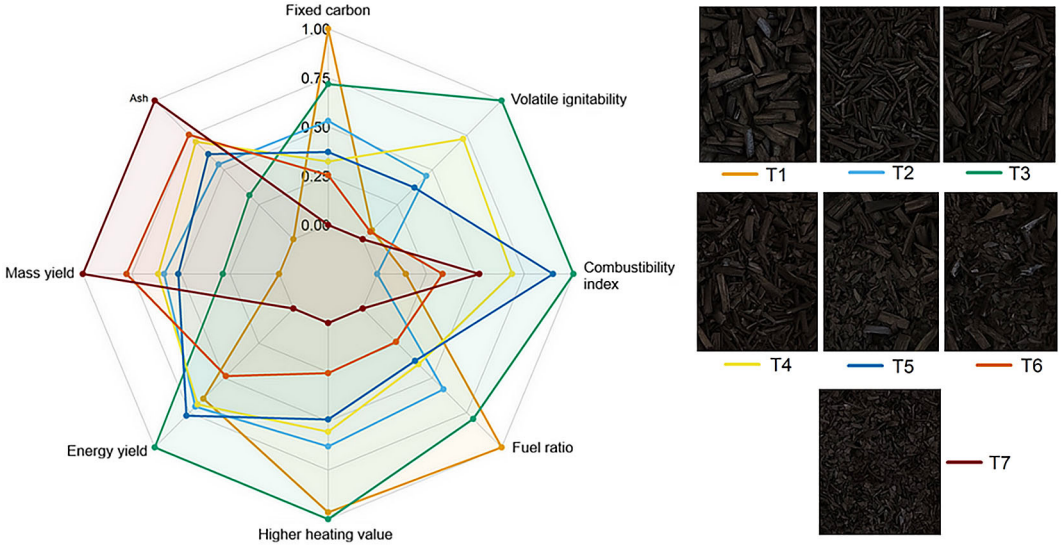

Figure 6. Profile of solid-fuel indicators for biochars from *Ficus benjamina*

the *Ficus benjamina* pruning biomass fractions was reflected in the relative performance of the biochars as solid fuels**.**

Normalized profile of solid-fuel indicators

Normalization of the eight indicators showed distinct treatment profiles (Figure 6). T3 presented high relative values of fixed carbon (FC), energy yield (EY), higher heating value (HHV), combustibility index (CI), and volatile ignitability (VI), while T1 stood out mainly in FC and fuel ratio (FR). In contrast, T7 showed the highest relative values of mass yield (Y) and ash, but the lowest of HHV, EY, FR, and VI. This pattern evidences a differentiated response between mass yield and several indicators associated with energy performance, so that a higher Y did not necessarily imply better fuel characteristics. The joint variation of yield, heating value, and proximate properties has also been observed during the thermochemical conversion of urban pruning residues (Paudel et al., 2025), while FC, volatile matter, HHV, and combustion indices have been used jointly to characterize biochars for energy purposes (Hadey et al., 2022). Consequently, the observed differences can be associated with the composition of the *Ficus benjamina* pruning biomass fractions and their mixtures. Figure 6 should be interpreted as a relative comparison indicator by indicator; the area enclosed by each profile does not represent an aggregate measure of performance, particularly because indicators such as mass yield, ash content, and FR have different implications in the evaluation of fuel.

CONCLUSIONS

The proportion of leaves, branches, and twigs in *Ficus benjamina* pruning residues significantly influenced the mass yield, proximate composition, and energy properties of biochars produced at 500 °C for 1 h. Formulations with a higher proportion of woody material generally exhibited superior energy characteristics; in particular, T3 achieved the highest HHV (25.50 MJ/kg), energy yield (47.95%), calorific value improvement (48.20%), combustibility index (9.40 MJ/kg), and volatile ignitability (23.51 MJ/kg). In contrast, T7 achieved the highest mass yield (37.01%) but showed the lowest HHV (18.06 MJ/kg), and energy yield (37.84%), demonstrating a trade-off between solid product recovery and energy quality. Differences in elemental composition, H/C and O/C ratios, functional groups, and ash content confirmed that the composition of the precursor biomass determined the final properties of the biochar. Overall, the results identify T3 as the formulation with the most favorable energy profile among those evaluated and support the thermochemical valorization of *Ficus benjamina* pruning residues as a feedstock for producing biochars with potential for energy applications.

REFERENCES

1. Abdullah, H., Mediaswanti, K., Wu, H. (2010). Biochar as a fuel: 2. Significant differences in fuel quality and ash properties of biochars from various biomass components of mallee trees. *Energy*

Fuels, *24*(3), 1972–1979. https://doi.org/10.1021/ef901435f'%5D

2. Anđelini, D., Cvitan, D., Prelac, M., Pasković, I., Černe, M., Nemet, I., Major, N., Ban, S. G., Užila, Z., Ferri, T. Z., Džakula, B. N., Petek, M., Ban, D., Palčić, I. (2023). Biochar from grapevine-pruning residues is affected by grapevine rootstock and pyrolysis temperature. *Sustainability*, *15*(6). https://doi.org/10.3390/su15064851
3. Ayaa, F., Oyedotun, K., Lubwama, M., Iwarere, S. A., Daramola, M. O., Kirabira, J. B. (2025). Production and characterization of densified briquettes from nanocomposite biochar-cellulose nanocrystal (biochar-CNC) reinforced with polyvinyl alcohol. *Waste and Biomass Valorization*, *16*(5). https://doi.org/10.1007/s12649-025-03005-9
4. Borges, A. D. S., Cardoso, M., Oliveira, M. (2025). Thermochemical evaluation of biochars properties from Portuguese agro-forestry residues for solid fuel applications. *Scientific Reports*, *16*(1), 1120. https://doi.org/10.1038/s41598-025-30809-5
5. Campos, P., Miller, A. Z., Knicker, H., Costa-Pereira, M. F., Merino, A., De la Rosa, J. M. (2020). Chemical, physical and morphological properties of biochars produced from agricultural residues: Implications for their use as soil amendment. *Waste Management*, *105*, 256–267. https://doi.org/10.1016/j.wasman.2020.02.013
6. Cao, X., Zhong, L., Peng, X., Sun, S., Li, S., Liu, S., Sun, R. (2014). Comparative study of the pyrolysis of lignocellulose and its major components: Characterization and overall distribution of their biochars and volatiles. *Bioresource Technology*, *155*, 21–27. https://doi.org/10.1016/j.biortech.2013.12.006
7. Cárdenas-Aguiar, E., Méndez, A., Gascó, G., Lado, M., Paz-González, A. (2024). The effects of feedstock, pyrolysis temperature, and residence time on the properties and uses of biochar from broom and gorse wastes. *Applied Sciences*, *14*(10), 4283. https://doi.org/10.3390/app14104283
8. Conag, A. T., Villahermosa, J. E. R., Cabatingan, L. K., Go, A. W. (2017). Energy densification of sugarcane bagasse through torrefaction under minimized oxidative atmosphere. *Journal of Environmental Chemical Engineering*, *5*(6), 5411–5419. https://doi.org/10.1016/j.jece.2017.10.032
9. de Jesus Paula, R., de Almeida Pereira, V., Latorre, F. L., Oliveira de Souza Nogueira, C., de Almeida, I. A., Freitas e Silva, P. A., Ferreira, O. E., de Lima, R. P., da Silva Bezerra, A. C., Machado, A. R. T. (2025). Pyrolysis converts urban pruning waste into biochar with soil and climate benefits. *Scientific Reports*, *15*(1), 45071. https://doi.org/10.1038/s41598-025-32360-9
10. Domingues, R. R., Trugilho, P. F., Silva, C. A., Melo, I. C. N. A. de, Melo, L. C. A., Magriotis, Z. M., Sánchez-Monedero, M. A. (2017). Properties of biochar derived from wood and high-nutrient biomasses with the aim of agronomic and environmental benefits. *PLoS ONE, 12*(5). https://doi.org/10.1371/journal.pone.0176884
11. Gao, Q., Zhang, T., Feng, Z., Yang, J., Ni, L., Hu, W., Liu, Z. (2022). Energy performances of molded charcoals from bamboo and Chinese fir blends: Influence of pyrolysis temperatures and residence times. *Industrial Crops and Products*, *177*, 114500. https://doi.org/10.1016/j.indcrop.2021.114500
12. Hadey, C., Allouch, M., Alami, M., Boukhlifi, F., Loulidi, I. (2022). Preparation and characterization of biochars obtained from biomasses for combustible briquette applications. *The Scientific World Journal*, *2022*, e2554475. https://doi.org/10.1155/2022/2554475
13. Ibitoye, S. E., Alam, M., Olayemi, O. A., Akinlabi, E. T., Sarkar, I., Mahamood, R. M., Jen, T.-C., Loha, C. (2025). Energy potential of biochar from slow pyrolysis of mixed tree leaves in a pilot-scale fixed-bed reactor. *International Journal of Renewable Energy Development*. *14*(5). https://ijred.cbiore.id/index.php/ijred/article/view/61253
14. Janu, R., Mrlik, V., Ribitsch, D., Hofman, J., Sedláček, P., Bielská, L., Soja, G. (2021). Biochar surface functional groups as affected by biomass feedstock, biochar composition and pyrolysis temperature. *Carbon Resources Conversion*, *4*, 36–46. https://doi.org/10.1016/j.crcon.2021.01.003
15. Kazimierski, P., Hercel, P., Suchocki, T., Smoliński, J., Pladzyk, A., Kardaś, D., Łuczak, J., Januszewicz, K. (2021). Pyrolysis of pruning residues from various types of orchards and pretreatment for energetic use of biochar. *Materials*, *14*(11), Article 11. https://doi.org/10.3390/ma14112969
16. Kujawska, J., Cel, W., Charmas, B., Szala, D. (2026). Effect of pyrolysis temperature on chemical structure and thermal stability of digestate-based biochar. *Energies*, *19*(4). https://www.mdpi.com/1996-1073/19/4/1043
17. Leng, S., Li, W., Han, C., Chen, L., Chen, J., Fan, L., Lu, Q., Li, J., Leng, L., Zhou, W. (2020). Aqueous phase recirculation during hydrothermal carbonization of microalgae and soybean straw: A comparison study. *Bioresource Technology*, *298*, 122502. https://doi.org/10.1016/j.biortech.2019.122502
18. Llanos, S. A. V., Gamarra, F. M. C., Collana, J. T. M., Scheineder, S. H., Chuquizuta, J. C. M., Mendoza, P. C., Quispea, A. P. B. (2023). Estimation of emission factors and ignitability index from the physicochemical characterization of *Ficus benjamina* for energy purposes. *Chemical Engineering Transactions*, *103*, 931-936. https://doi.org/10.3303/CET23103156
19. Llanos, S. A. V., Purihuaman, M. S., Scheineder, S. H., Cuellar, M. C. V., Sipion, K. del P. R., Borrero, E. C. C., Farfan, C. R. C., Quispe, A. P. B. (2026). Biochar from pruned *Ficus benjamina* branches:

Carbonization temperature effects on properties and applicability as solid biofuel and soil amendment applications. *Journal of Ecological Engineering*, *27*(1). https://doi.org/10.12911/22998993/209781

20. Lu, Q., Xie, W., Hu, B., Liu, J., Zhao, W., Zhang, B., Wang, T. (2021). A novel interaction mechanism in lignin pyrolysis: Phenolics-assisted hydrogen transfer for the decomposition of the *β*-O-4 linkage. *Combustion and Flame*, *225*, 395–405. https://doi.org/10.1016/j.combustflame.2020.11.011
21. Luthfi, N., Fukushima, T., Wang, X., Takisawa, K. (2024). Hydrochar as an alternative to coal: a comparative study of lignocellulosic and nonlignocellulosic biomass. *Resources*, *13*(4). https://doi.org/10.3390/resources13040049
22. Mafu, L. D., Neomagus, H. W. J. P., Everson, R. C., Strydom, C. A., Carrier, M., Okolo, G. N., & Bunt, J. R. (2017). Chemical and structural characterization of char development during lignocellulosic biomass pyrolysis. *Bioresource Technology*, *243*, 941–948. https://doi.org/10.1016/j.biortech.2017.07.017
23. Mbugua Nyambura, S., Li, C., Li, H., Xu, J., Wang, J., Zhu, X., Feng, X., Li, X., Bertrand, G. V., Ndiithi Ndumia, J., Lai Fui Chin, B. (2023). Microwave co-pyrolysis of kitchen food waste and rice straw: Effects of susceptor on thermal, surface, and fuel properties of biochar. *Fuel*, *352*, 129093. https://doi.org/10.1016/j.fuel.2023.129093
24. Minatre, K. L., Arienzo, M. M., Moosmüller, H., Maezumi, S. Y. (2024). Charcoal analysis for temperature reconstruction with infrared spectroscopy. *Frontiers in Earth Science*, *12*. https://doi.org/10.3389/feart.2024.1354080
25. Park, S., Kim, S. Y., Oh, K. C., Kim, S. J., Paudel, P. P., Park, D. S., Kang, K. S., Ryu, S. H., Kim, D. H. (2025). Fuel properties of torrefied pellets from maize residues and cocopeat byproducts. *Biomass*, *5*(4). https://www.mdpi.com/2673-8783/5/4/59
26. Paudel, P. P., Park, S., Oh, K. C., Kim, S. J., Kim, S. Y., Kang, K. S., Kim, D. H. (2025). Energy recovery from Ginkgo biloba urban pruning wastes: Pyrolysis optimization and fuel property enhancement for high-grade charcoal productions. *Biofuels, Bioproducts and Biorefining*, *19,* 2246-2260. https://doi.org/10.1002/bbb.70017
27. Pérez-Arévalo, J. J., Velázquez-Martí, B. (2018). Evaluation of pruning residues of Ficus benjamina as a primary biofuel material. *Biomass and Bioenergy*, *108*, 217–223. https://doi.org/10.1016/j.biombioe.2017.11.017
28. Petricoski, S. M., Feiden, A., Oliveira, A. F. de, Tokura, L. K., Siqueira, J. A. C., Bonassa, G., Zilli, B. M., Gentelini-Marquez, D. P., Souza, S. N. M. de, Feiden, C. A., Feiden, E. A., Martinez, A. da S. (2020). Briquettes produced with a mixture of urban pruning waste, glycerin and cassava processing residue. *Journal of Agricultural Science*, *12*(6), p158. https://doi.org/10.5539/jas.v12n6p158
29. Prelac, M., Palčić, I., Cvitan, D., Anđelini, D., Repajić, M., Ćurko, J., Kovačević, T. K., Goreta Ban, S., Užila, Z., Ban, D., Major, N. (2023). Biochar from grapevine pruning residues as an efficient adsorbent of polyphenolic compounds. *Materials*, *16*(13), 4716. https://doi.org/10.3390/ma16134716
30. Qian, C., Li, Q., Zhang, Z., Wang, X., Hu, J., Cao, W. (2020). Prediction of higher heating values of biochar from proximate and ultimate analysis. *Fuel*, *265*, 116925. https://doi.org/10.1016/j.fuel.2019.116925
31. Qiu, L., Li, C., Zhang, S., Wang, S., Li, B., Cui, Z., Tang, Y., Hu, X. (2023). Distinct property of biochar from pyrolysis of poplar wood, bark, and leaves of the same origin. *Industrial Crops and Products*, *202*, 117001. https://doi.org/10.1016/j.indcrop.2023.117001
32. Saletnik, B., Bajcar, M., Saletnik, A., Zaguła, G., Puchalski, C. (2021). Effect of the pyrolysis process applied to waste branches biomass from fruit trees on the calorific value of the biochar and dust explosivity. *Energies*, *14*(16). https://www.mdpi.com/1996-1073/14/16/4898
33. Santos, S. M., Gonçalves, M., Brito, P., Nobre, C. (2026). Char Produced from waste and biomass blended pellets: comprehensive thermochemical behavior assessment. *Environments*, *13*(2). https://doi.org/10.3390/environments13020119
34. Shahbaz, M., AlNouss, A., Parthasarathy, P., Abdelaal, A. H., Mackey, H., McKay, G., Al-Ansari, T. (2020). Investigation of biomass components on the slow pyrolysis products yield using Aspen Plus for techno-economic analysis. *Biomass Conversion and Biorefinery*, *12*(3), 669–681. https://doi.org/10.1007/s13399-020-01040-1
35. Silva, M. P., Moyano, E. L., Scopel, A. L. (2017). Potential applications of biochar and terpene-enriched bio-oil produced from a semi-arid native Asteraceae. *Journal of Analytical and Applied Pyrolysis*, *126*, 39–49. https://doi.org/10.1016/j.jaap.2017.06.026
36. Sun, X., Shan, R., Li, X., Pan, J., Liu, X., Deng, R., Song, J. (2017). Characterization of 60 types of Chinese biomass waste and resultant biochars in terms of their candidacy for soil application. *GCB Bioenergy*, *9*(9), 1423–1435. https://doi.org/10.1111/gcbb.12435
37. Taboada-Ruiz, L., Pardo, R., Ruiz, B., Díaz-Somoano, M., Calvo, L. F., Paniagua, S., Fuente, E. (2024). Progress and challenges in valorisation of biomass waste from ornamental trees pruning through pyrolysis processes. Prospects in the bioenergy sector. *Environmental Research*, *249*, 118388. https://doi.org/10.1016/j.envres.2024.118388
38. Tomczyk, A., Sokołowska, Z., Boguta, P. (2020). Biochar physicochemical properties: Pyrolysis temperature and feedstock kind effects.

Reviews in Environmental Science and Bio/Technology, *19*(1), 191–215. https://doi.org/10.1007/s11157-020-09523-3

39. Valdebenito, F., Ramírez-Álvarez, R., Alexandra Muñoz, M., Pecchi, G., Canales, R., Ormazabal, S., Muñoz, R., Alejandro-Martín, S., Quero, F., Adam, R., Cifuentes, G., Flavio Espinoza-Monje, J., Azócar, L. (2024). Biomass characterization and solvent extraction as tools to promote phenol production from urban pruning. *Fuel*, *362*, 130830. https://doi.org/10.1016/j.fuel.2023.130830
40. Wang, J. (2026). Species and functional trait determinants of biochar carbon retention: insights from uniform smoldering experiments. *Forests*, *17*(1), 116. https://doi.org/10.3390/f17010116
41. Waters, C. L., Janupala, R. R., Mallinson, R. G., Lobban, L. L. (2017). Staged thermal fractionation for segregation of lignin and cellulose pyrolysis products: An experimental study of residence time and temperature effects. *Journal of Analytical and Applied Pyrolysis*, *126*, 380–389. https://doi.org/10.1016/j.jaap.2017.05.008
42. Yang, H., Gong, M., Hu, J., Liu, B., Chen, Y., Xiao, J., Li, S., Dong, Z., Chen, H. (2020). Cellulose pyrolysis mechanism based on functional group evolutions by two-dimensional perturbation correlation infrared spectroscopy. *Energy & Fuels*, *34*(3), 3412–3421. https://doi.org/10.1021/acs.energyfuels.0c00134
43. Yang, X., Kang, K., Qiu, L., Zhao, L., Sun, R. (2020). Effects of carbonization conditions on the yield and fixed carbon content of biochar from pruned apple tree branches. *Renewable Energy*, *146*, 1691-1699. https://doi.org/10.1016/j.renene.2019.07.148
44. Yang, X., Wang, H., Strong, P. J., Xu, S., Liu, S., Lu, K., Sheng, K., Guo, J., Che, L., He, L., Ok, Y. S., Yuan, G., Shen, Y., Chen, X. (2017). Thermal properties of biochars derived from waste biomass generated by agricultural and forestry sectors. *Energies*, *10*(4), 469. https://doi.org/10.3390/en10040469
45. Yao, B., Xiao, T., Jie, X., Gonzalez-Cortes, S., Edwards, P. P. (2018). H2–rich gas production from leaves. *Catalysis Today, SI: Decarbonising Fossil Fuel*, *317*, 43-49. https://doi.org/10.1016/j.cattod.2018.02.048
46. Zhang, S., Jia, X., Wang, X., Chen, J., Cheng, C., Jia, X., Hu, H. (2024). Using the conditional process analysis model to characterize the evolution of carbon structure in taxodium ascendens biochar with varied pyrolysis temperature and holding time. *Plants*, *13*(3). https://www.mdpi.com/2223-7747/13/3/460
47. Zhao, S.-X., Ta, N., Wang, X.-D. (2017). Effect of temperature on the structural and physicochemical properties of biochar with apple tree branches as feedstock material. *Energies*, *10*(9), Article 9. https://doi.org/10.3390/en10091293